Turbulencelike scaling in polymer interfaces

I. J. Lee and Euldoo Park

Department of Physics, Research Institute of Physics and Chemistry, Chonbuk National University, Jeonju, 561-756, Republic of Korea

(Received 12 August 2011; revised manuscript received 25 January 2013; published 11 March 2013)

The spatial structure and statistical properties of polymer interfaces grown by vapor deposition polymerization have been studied in the context of fluid turbulence. The extended self-similarity present in the correlation functions of the polymer interface uncovers two types of multiscaling for different spatial scales. The relative qth-order scaling exponents and the probability distribution functions of the height gradient display intermittent height fluctuations, which lead to spatial multiscaling analogous to the velocity fluctuations in turbulent fluid.

DOI: 10.1103/PhysRevE.87.032402 PACS number(s): 81.15.Aa, 68.55.−a, 05.40.−a, 47.27.−i

I. INTRODUCTION

Multifractality has been an important concept in the understanding of a wide class of far-from-equilibrium systems in which invariance under simple scale transformation fails. In particular, the idea of multifractality played a significant role in capturing essential features of intermittency in fully developed turbulence [1–3]. The concept of multifractality was extended to self-affine fractals [4] and has been applied for a specific class of real growth fronts called multi-affine surfaces. These kinds of growing surfaces include vacuum-deposited porous films, slow combustion of paper, two-phase fluid flow in porous media, and rupture lines in paper [5–8]. So far, the spatial multiscaling known to exist in a few real growth systems has been understood in association with large fluctuations of height gradients, which are introduced through a power-law noise distribution [9]. Since intermittent height fluctuations of rough interfaces were first noticed by Krug [10] in the context of fluid turbulence more than a decade ago, a one-dimensional limited mobility model of epitaxial growth and a similar class of growth models have been studied in detail [11–13]. However, this phenomenon of turbulent interface never has been confirmed in a real growth system. In this report, we present clear experimental evidence that vapor deposited polymer films have spatial structure and statistical properties which, at the interfaces, are remarkably similar to those of the velocity fluctuations in turbulent fluids [14,15]. Moreover, surprisingly rich multiscaling behaviors revealed by analysis based on the extended self-similarity provide interesting insight into the interplay between the phenomena of multiscaling and intermittency in close relation with the anomalous kinetic roughening of the polymer interface [16].

In fully developed turbulence, the scaling behavior of small-scale fluctuations are observed in a spatial scale r called the inertial range, $\eta \ll r \ll L$, in which the average energy transfer rate is the only relevant quantity; this implies that neither the energy injection at scale L nor dissipation by molecular viscosity below a scale of η takes place in this range. The qth-order velocity structure functions are defined in the inertial range as

$$S_q(r) = \langle [u(\mathbf{x}+\mathbf{r}) - u(\mathbf{x})]^q \rangle \sim r^{\zeta'_q}, \tag{1}$$

where $[u(\mathbf{x}+\mathbf{r}) - u(\mathbf{x})]$ is the velocity difference between two spatial locations which are a distance $\mathbf{r}$ apart, and the brackets $\langle \cdots \rangle$ denote the spatial average. The exponents ζ'_q significantly deviate from the classical theory of Kolmogorov (i.e., $\zeta'_q = q/3$) [17] due to the presence of strong bursts in the energy dissipation, which is known as the intermittency phenomenon. Intermittent energy transfer toward the dissipative scale in fully developed turbulence is also related to the statistical properties of the velocity gradient. It is well known from multifractal notions of turbulence that the probability distribution function (PDF) of the velocity gradient is given by stretched exponentials [15,18,19] whose forms depend strongly on the Reynolds number [20].

For multi-affine surfaces, the fluctuations of interface height $h(\mathbf{x})$ are characterized by the qth root of the qth-order height-difference correlation function for a fixed time as [10]

$$G_q(r) = \langle |h(\mathbf{x}+\mathbf{r}) - h(\mathbf{x})|^q \rangle^{1/q} = \xi^{\alpha_q} r^{\zeta_q} f_q(r/\xi), \tag{2}$$

where ξ is the lateral correlation length whose length scale is determined by the deposition time t through $\xi = t^{1/z}$ with the dynamic exponent z. The scaling function behaves as $f_q(r/\xi) = \text{const}$ when $r \ll \xi$ and $f_q(r/\xi) = (r/\xi)^{-\zeta_q}$ when $r \gg \xi$. Therefore, if the separation distance r between the measured heights is much smaller than the lateral correlation length (i.e., $r \ll \xi$) the correlation function is given by

$$G_q(r) \sim r^{\zeta_q}. \tag{3}$$

A close similarity between the scaling properties of height fluctuations in growth surface and those of the velocity fluctuations in fully developed turbulence can be realized when the role of the velocity field $u(\mathbf{x})$ in fully developed turbulence is played by the height function $h(\mathbf{x})$ [10,13]. Notice that the correlation length ξ setting the spatial scale of the scale-invariant regime effectively functions as the Reynolds number in turbulence.

II. EXPERIMENT

Poly(chloro-p-xylylene) (PPX-C) films were deposited on naturally grown SiO_2 layers on Si substrates (SiO_2/Si substrates) in a custom-built chemical vapor deposition reactor at room temperature. Dimer molecules (dichloro-di-p-xylylene) were sublimed at 120 °C and then cracked into monomers in the pyrolysis furnace at 660 °C. The monomer vapor was subsequently condensed and polymerized on naturally grown SiO_2/Si substrates at room temperature in the deposition chamber. Spectroscopic ellipsometry was used to determine the film thickness d. The surface morphology was measured using atomic force microscopy (AFM) (XE-100, Park systems) in a noncontact mode. The half-cone angle at the single-

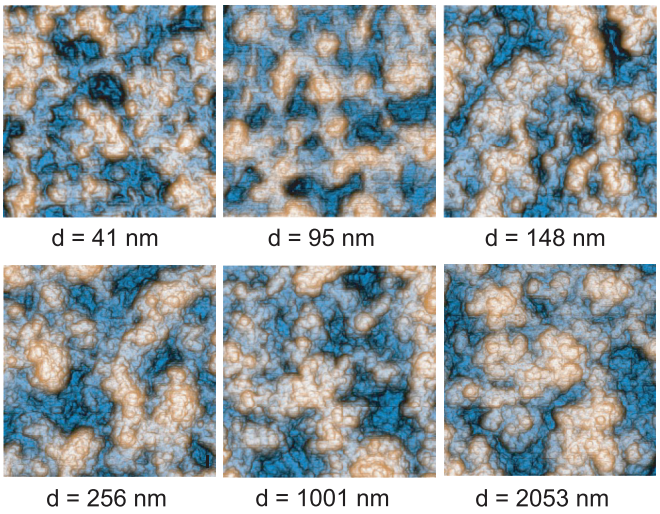

FIG. 1. (Color online) Topographic AFM images of PPX-C films at various film thicknesses. For each image, a scan area of $1 \times 1\ \mu m^2$ was taken with a 512×512 pixel resolution.

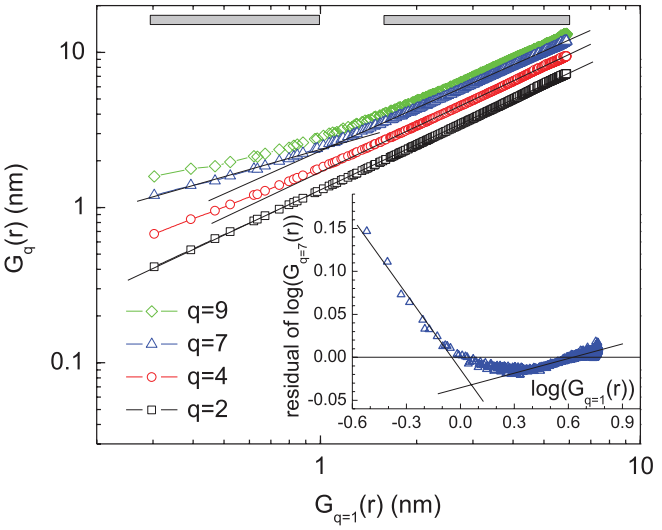

FIG. 2. (Color online) Log-log (with base 10) plot of $G_q(r)$ vs $G_{q=1}(r)$ for $q = 2$, 4, 7, and 9 at film thickness $d = 2053$ nm. Inset displays the residual of $\log_{10}(G_{q=7}(r))$ resulting from a linear best fit for the entire range. Gray bars indicate the range used for estimating exponents. Lines through data are guides for the eyes.

crystal silicon AFM tip apex (NCHR, nanosensors) was approximately 10 deg, and the typical tip radii were smaller than 7 nm. Further details of the experimental methods can be found in our recent reports [16,21]. Representative AFM images taken at various growth stages are shown in Fig. 1. Data analyses were performed on the two-dimensional AFM images of a scan area of $1 \times 1\ \mu m^2$ taken with 512×512 pixels. The q-dependent correlation functions $G_q(r)$ were calculated by direct two-dimensional averaging of the AFM images, which include average over all 512×512 data points and all directions of $\mathbf{r} = (r_x, r_y)$ for given length $r = |\mathbf{r}|$.

III. RESULTS AND DISCUSSION

In addition to the intermittency phenomenon, in regard to the velocity structure function, it is of note that regime of scale invariance is significantly extended over a wider spatial range when different order structure functions $|S_p(r)|$ and $|S_q(r)|$ are plotted against each other even if the power law in the spatial scale [Eq. (1)] is not developed at a small Reynolds number [22]. This effect, called extended self-similarity (ESS), provides a significant improvement when it comes to finding the relative scaling exponents (i.e., ζ'_p/ζ'_q). The same scheme of ESS analysis is applied to all the qth-moment correlation functions $G_q(r)$, which were obtained from wide range of film thicknesses. An example of our ESS analysis is shown in Fig. 2, which demonstrates a behavior typical of the growth regime where an additional power law appears in a small-r length scale. As shown in the trace of $q = 2$, the self-similarity of the height fluctuation extends for the entire spatial range beyond the conventionally defined length scale ($r \ll \xi$) in which Eq. (3) is normally applicable. Notice from Fig. 3(a) displaying $g_q(r)$ vs r that an apparent power law is limited in the small length scale up to $r \sim 10$–20 nm. It is also interesting to notice in Fig. 2 that a clear deviation from the background scaling behavior is apparent below $G_{q=1}(r) \sim 1.6$, which corresponds $r \sim 20$ nm in length scale. The deviations grow larger as the qth moment increases. Considering the strongly

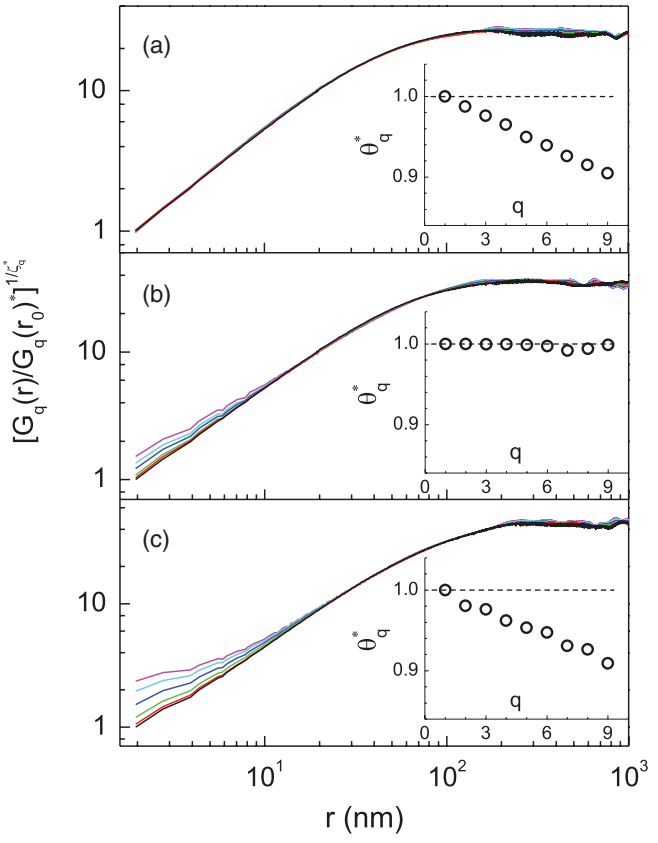

FIG. 3. (Color online) Log-log (with base 10) plot of the scaling function $g_q(r)$ vs r at various film thicknesses: (a) $d = 13.6$ nm, (b) $d = 41.0$ nm, and (c) $d = 2053$ nm. In each main panel starting from the bottom trace and going up, $q = 1$, 2, 3, 5, 7, and 9. The inset in each panel shows the relative exponents θ^*_q as a function of q. The dotted line indicates expected exponents for self-affine fractal.

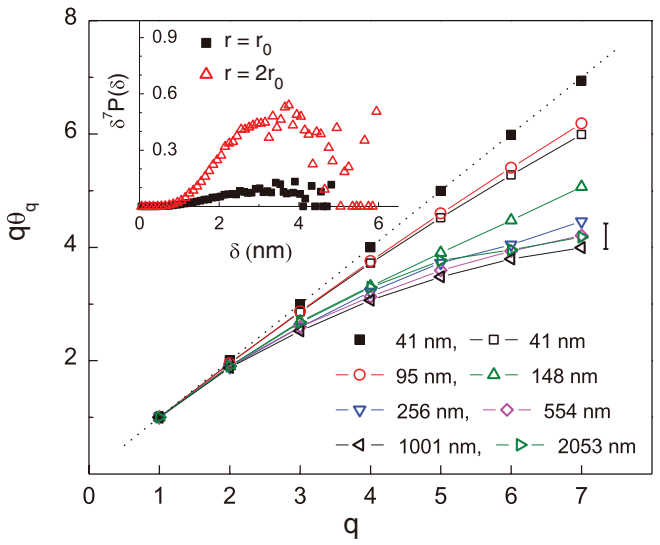

FIG. 4. (Color online) Relative qth order scaling exponents $q\theta_q$ plotted vs q. The dashed line marks a slope of 1. The inset shows the integrand $\delta^7 P(\delta)$ vs δ at two different separations, $r = r_0$ (solid squares) and $r = 2r_0$ (open triangles).

non-Gaussian shape of the PDF of height gradient in the relevant grown regime (see Figs. 5 and 6), we are certain that the q-dependent deviations in the small-r scale are most likely due to the development of multiscaling [15,18,19], which is usually characterized by q-dependent scaling exponents. However, it is not straightforward to determine the relative qth-order exponents, that is, the slope of each trace in the ESS plot. The quality of a linear regression for the entire trance of the seventh moment is illustrated in the inset of Fig. 2 in which the residual (i.e., the measured value – the fit value) of $\log_{10}(G_{q=7}(r))$ vs $\log_{10}(G_{q=1}(r))$ is displayed for the whole range. The base line indicates a slope of 0.877. Two clear trends in the residual plot allow us to fit the data in two different scaling regions separately, small r below $G_{q=1}(r) = 1$ and large-r length scale above $G_{q=1}(r) = 1.6$, which correspond to spatial scales $r = 10$ nm and 20 nm, respectively [23]. We note that the examination of the scaling properties in the large-r length scale would not be possible without the application of ESS. The relative scaling exponents in the large-r region θ_q^* (i.e., $\zeta_q^*/\zeta_{q=1}$) are determined precisely from the ESS plot, which reads as $\theta_2^* = 0.987 \pm 0.001, \theta_4^* = 0.962 \pm 0.001$, $\theta_7^* = 0.927 \pm 0.001$, and $\theta_9^* = 0.907 \pm 0.002$. The second set of relative exponents in the small-r scale θ_q is obtained as $\theta_2 = 0.95 \pm 0.01$, $\theta_4 = 0.82 \pm 0.01$, $\theta_7 = 0.60 \pm 0.02$, and $\theta_9 = 0.48 \pm 0.02$. Figure 4 summarizes the qth-order scaling exponents $q\theta_q$ obtained in the small-r spatial scale using the same scheme of ESS analysis (i.e., a type of Fig. 2) on the correlation functions at various film thicknesses.

Some of the interesting results obtained from the ESS analysis include an indication that the q-dependent scaling behavior appears to subsist in the large-r spatial scale and the scaling behavior exhibits interesting progressions in close relation with the known growth regimes of polymer films [16]. In Fig. 3, we show the scaling function $g_q(r) \equiv [G_q(r)/G_q(r_0)^*]^{1/\zeta_q^*}$ vs r at various film thicknesses. The value $G_q(r_0)^*$ is an average height gradient at $r_0 = 1.95$ nm in the absence of (or neglecting) the multiscaling in the small-r scaling region. The exponents ζ_q^* are obtained from the relation $\zeta_q^* = \theta_q^* \zeta_{q=1}$, once $\zeta_{q=1}$ is directly measured from the correlation function $G_{q=1}(r)$. As previously noted by Kundagrami *et al.* [13], the property of ESS ensures the presence of a q-independent scaling function, i.e., $f_q(r/\xi) \sim f(r/\xi)^{\zeta_q^*}$. Thus, the implication of ESS in association with Eq. (2) suggests that the plot of the scaling function $g_q(r)$ vs r for various qth moments would collapse into a single curve depending on the integrity of estimate of the scaling exponents θ_q^* in the large-r scale. Displayed in Fig. 3 is a representative scaling function for the large-r spatial scale in three different growth stages of polymer films [16]: in panel (a) we show scaling function in initial growth regime before the substrate is fully covered ($d \leqslant 14$ nm), panel (b) is obtained for a valley-filling regime (14 nm $< d \leqslant 150$ nm), and panel (c) exhibits a behavior typical of the continuous growth regime ($d > 150$ nm). The inset of each panel displays the q-dependent scaling exponents θ_q^* which are determined from the ESS analysis and used to construct the scaling functions. The presence of ESS in the large-r scale as well as the integrity of the related scaling exponents determined from the type of Fig. 2 are manifested nicely by the collapse of the q-dependent scaling functions $g_q(r)$ into a single curve. The standard fitting error involved in the estimate of θ_q^* is generally not bigger than the size of symbols in the inset. Note that in the large-r scaling regime, the presence of a single scaling function with q-dependent (or q-independent) scaling exponents θ_q^* is clear evidence for multiscaling (or self-affine scaling) behavior.

In the regime (a), a nearly perfect data collapse with the q-dependent exponents θ_q^* is observed for the entire spatial scale. Data suggest that the multi-affine (or multifractal) interface persists up to $r \sim \xi$, which is similar to what had been found in the epitaxial growth models with limited surface mobility [10,13]. In regime (b), as indicated by the deviations from the data collapse, multiscaling behavior develops in the small-r length scale, while a characteristic of self-affine interfaces appears in the large-r scale as indicated by the exponents θ_q^*, which remain nearly the same for the different qth moments. In the continuous growth regime (c), the property of multi-affine interfaces emerges again in large-r scales in addition to the small-r multiscaling. Two distinctive spatial multiscalings which are turned on and off depending on the growth stage of polymer film must be responsible for the anomalous kinetic roughening observed previously in the polymer interface [16]. The dependence of θ_q^* is almost identical in both growth regimes (a) and (c), which suggests that the anomalous super-roughening process, known to occur in both growth regimes [16], is closely related with the large-r scale multiscaling. The observation may provide an additional constraint for previous conjecture on the condition for the super-rough interface [24].

Uncertainty associated with the measurements of high moments of the height gradient increases as tails of a PDF extend to larger amplitude [14]. In the inset of Fig. 4, we show the integrand in the definition of the seventh moment at the separation length r_0 and $2r_0$ at $d = 2053$ nm. At the seventh moment, the integrand has decreased at the largest height gradient (δ) to a level at which its moment can be

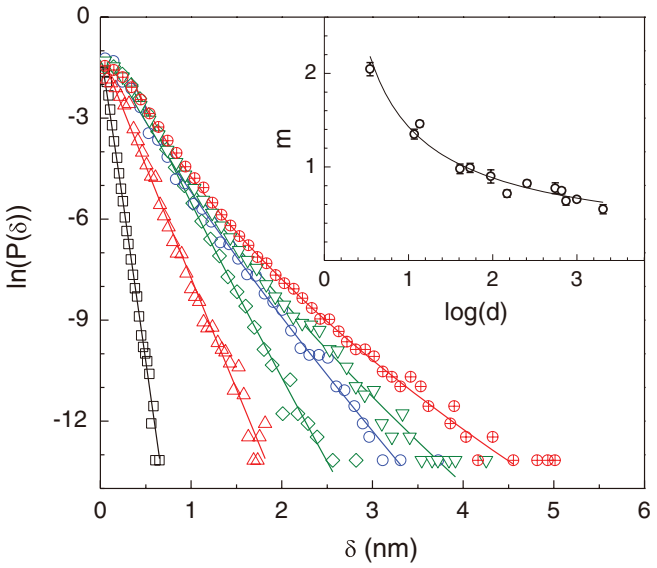

FIG. 5. (Color online) Natural log-linear plot of the PDF of height gradient $\ln P(\delta)$ vs δ for film thicknesses, $d = 0$ (bare substrate), 41, 95, 256, 659, and 2053 nm, from left to right. Inset shows the stretched exponential parameter m plotted vs $\log_{10}(d)$.

estimated within reasonable accuracy [25]. Relative q-order scaling exponents $q\theta_q$ up to seventh order for various film thickness are displayed as open symbols in Fig. 4. The solid squares representing $q\theta_q^*$ for a film at $d = 41$ nm provide a reference curve for a self-affine fractal. Intermittent height fluctuations manifest themselves by clear deviations from the linear self-affine slope. We note that the behavior of q-dependent relative exponents can be grouped into two regimes, i.e., the valley-filling regime and the continuous growth regime, roughly separated by a film thickness $d \sim$ 100 nm. The fairy universal behavior of $q\theta_q$ in each growth stage of the polymer film, which is in stark contrast with the

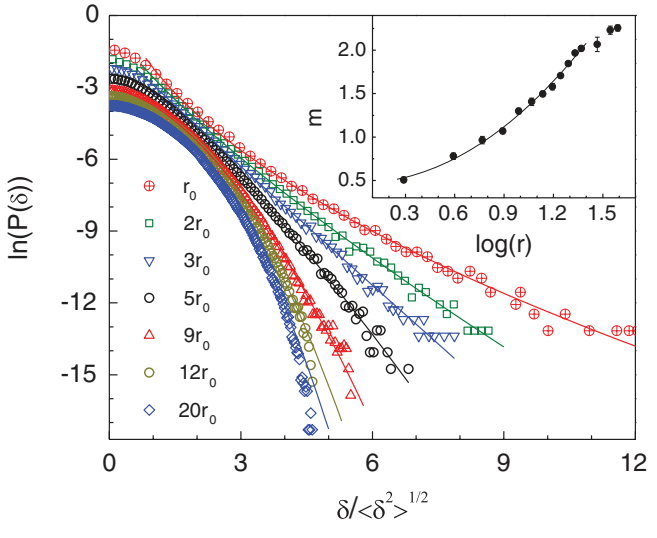

FIG. 6. (Color online) PDF of height gradient for various separation lengths at film thickness $d = 2053$ nm. Lines through data points are obtained from a stretched exponential fit. Inset displays the stretching parameter m as a function of $\log_{10}(r)$.

previous report regarding the vacuum deposited CaF_2 films [5], can be understood consistently in relation with the role of the Reynolds numbers played in the scaling exponents of fluid turbulence. The discrepancies in the scaling exponents from different films at the same growth stage grow larger as the qth moments increase, which is likely associated with the overall uncertainties involved in the estimate. Error bar at the seventh moment shows a variation of $\pm 5\%$.

The small-scale intermittent height fluctuations can also be characterized by the PDF of nearest-neighbor height gradient $P(\delta)$, which is displayed in Fig. 5. Data were taken at various film thicknesses. As the figure shows, the distributions of the height gradient are very well described by the distribution function of a stretched exponential, that is, $P(\delta) \sim \exp(-a\delta^m)$, where $\delta = |h(\mathbf{x} + r_0) - h(\mathbf{x})|/r_0$. We note that a stretched exponential provides good working approximations to typical experimental data for the tails of the PDF of velocity increments [19]. The solid lines through the data points are from the best fit with the stretching parameter m displayed in the inset. The PDF obtained from the naturally grown SiO_2 surface (bare substrate) is accurately described by an exponential function ($m = 1$). A Gaussian distribution ($m = 2$) develops in the tail section of the PDF, as polymer islands grow on the substrate (not shown in the figure). When the substrate is nearly covered at $d \sim 14$ nm, the shape of PDF becomes fit between Gaussian and exponential function. Multiscaling in a small-r scale occurs only after the substrate is fully covered, at which the PDF of the height gradient is strongly non-Gaussian (i.e., $m \leqslant 1$). The evolution in the shape of the PDF of height gradient as a function of $\log_{10}(d)$ is shown in the inset. The solid line through the data points is from a power law fit $m \sim (\log_{10}(d))^{-\gamma}$ with $\gamma = 0.70 \pm 0.04$. The fact that m follows a power law as a function of $\log_{10}(d)$ is consistent with the Reynolds number dependence of the stretching parameter proposed by Lohse and Grossmann in the context of fluid turbulence [20], which seems to confirm the presence of one-to-one correspondence between the correlation length of growing interface and the Reynolds number of turbulent fluid as expected.

The study of the scaling properties of the correlation function $G_q(r)$ using the collection of moments has a few limitations due to its small scaling range and large uncertainty at high order of moments. A better strategy based on the multifractal picture of turbulence dynamics is to examine the PDF of height difference [14] as displayed in Fig. 6. Data show that as the separation length r increases, the shape of PDFs evolves from square-root exponential for $r = r_0$ to Gaussian for $r \sim 11r_0$. Notice that the separation length $r \sim 11r_0$ is consistent with the length scale $r \sim 20$ nm at which the small-r multiscaling disappears in the scaling function displayed in Fig. 3(c). As the separation increases above $r = 12r_0$, the tail section of the PDFs deviates from Gaussian distribution due to an increasing number of rare events with large height difference, which is likely responsible for the large-r scale multiscaling. The structural and statistical properties of the large-r multiscaling seem different from those of the small-r multiscaling. The mechanisms leading to the formation of height fluctuations in the small-r scale, similar to the velocity fluctuations in fluid turbulence, would be an interesting subject

in its own right which is beyond the current scope of our discussion.

IV. CONCLUSION

We have studied the spatial structure and statistical properties of polymer interfaces in the context of fluid turbulence. The similarities between these two seemingly very different nonequilibrium systems are found to extend beyond what has been previously observed in real two-dimensional growth systems. The qth-order scaling exponents displaying clear deviation from a self-affine slope, and the characteristic progressions in the shape of the PDF of the height gradient for the separation lengths and for the film thicknesses are taken as decisive signatures of turbulencelike interfaces formed by vapor deposition polymerization. Interestingly, on the polymer interfaces, two distinctive multiscaling are discovered in different spatial scales, which are turned on and off depending on the growth stages of polymer film. These rich scaling properties should provide a rare glimpse into the interplay between the phenomena of multiscaling and intermittency which result in the known unusual kinetic roughening of polymer interface.

ACKNOWLEDGMENTS

We thank Hyunsoo Kim for helpful discussions. This work was supported by Korea Research Foundation Grant No. KRF-2008-313-C00336 and by National Research Foundation of Korea Grant No. NRF-2011-0011944.

[1] U. Frisch and G. Parisi, in *Turbulence and Predictability in Geophysical Fluid Dynamics and Climate Dynamics*, edited by M. Ghil, R. Benzi, and G. Parisi (North-Holland, Amsterdam, 1985).
[2] R. Benzi, G. Paladin, G. Parisi, and A. Vulpiani, J. Phys. A: Math. Gen. **17**, 3521 (1984).
[3] For a recent review, see G. Boffetta, A. Mazzino, and A. Vulpiani, J. Phys. A: Math. Theor. **41**, 363001 (2008).
[4] A.-L. Barabasi and T. Vicsek, Phys. Rev. A **44**, 2730 (1991).
[5] D. R. Luhman and R. B. Hallock, Phys. Rev. Lett. **92**, 256102 (2004).
[6] M. Myllys, J. Maunuksela, M. J. Alava, T. Ala-Nissila, and J. Timonen, Phys. Rev. Lett. **84**, 1946 (2000).
[7] V. K. Horvath, F. Family, and T. Vicsek, Phys. Rev. Lett. **67**, 3207 (1991).
[8] E. Bouchbinder, I. Procaccia, S. Santucci, and L. Vanel, Phys. Rev. Lett. **96**, 055509 (2006).
[9] A.-L. Barabasi, R. Bourbonnais, M. Jensen, J. Kertesz, T. Vicsek, and Y. C. Zhang, Phys. Rev. A **45**, R6951 (1992).
[10] J. Krug, Phys. Rev. Lett. **72**, 2907 (1994).
[11] S. Das Sarma, C. J. Lanczycki, R. Kotlyar, and S. V. Ghaisas, Phys. Rev. E **53**, 359 (1996).
[12] C. Dasgupta, J. M. Kim, M. Dutta, and S. DasSarma, Phys. Rev. E **55**, 2235 (1997).
[13] A. Kundagrami, C. Dasgupta, P. Punyindu, and S. Das Sarma, Phys. Rev. E **57**, R3703 (1998).
[14] F. Anselmet, Y. Cagne, E. J. Hopfinger, and R. A. Antonia, J. Fluid Mech. **140**, 63 (1984).
[15] A. Vincent and M. Meneguzzi, J. Fluid Mech. **225**, 1 (1991).
[16] I. J. Lee, M. Yun, S.-M. Lee, and J.-Y. Kim, Phys. Rev. B **78**, 115427 (2008).
[17] A. N. Kolmogorov, C. R. Acad. Sci. URSS **30**, 301 (1941).
[18] R. Benzi and L. Biferale, G. Paladin, A. Vulpiani, and M. Vergassola, Phys. Rev. Lett. **67**, 2299 (1991).
[19] P. Kailasnath, K. R. Sreenivasan, and G. Stolovitzky, Phys. Rev. Lett. **68**, 2766 (1992).
[20] S. Grossmann and D. Lohse, Europhys. Lett. **21**, 201 (1993); D. Loshe and S. Grossmann, Phys. A (Amsterdam, Neth.) **194**, 519 (1993).
[21] I. J. Lee and Euldoo Park, J. Phys. Soc. Jpn. **80**, 124602 (2011).
[22] R. Benzi, S. Ciliberto, R. Tripiccione, C. Baudet, F. Massaioli, and S. Succi, Phys. Rev. E **48**, R29 (1993); R. Benzi, S. Ciliberto, C. Baudet, and G. R. Chavarria, Phys. D (Amsterdam, Neth.) **80**, 385 (1995).
[23] We note that the fitting error depends strongly on the fitting range due to the transition regime existing between the length scale $r = 10$ and 20 nm. Within the fitting range we adapted, the standard error is given, at most (at $q = 7$), about $\pm 3\%$ in the small-r scaling region.
[24] N.-N. Pang and W.-J. Tzeng, Phys. Rev. E **61**, 3559 (2000).
[25] The uncertainty in the estimate of the correlation function significantly reduces as the spatial separation increases. For example, at the beginning of the large-r scaling region (i.e., $r = 10r_0$), a reasonable accuracy (within $\pm 5\%$ error) is achieved at the 11th moment.